corrected by R Smith

Conf-751125--104

MASTER

STRESS ANALYSIS OF PLT COIL

J. Frankenberg
Plasma Physics Laboratory, Princeton University
Princeton, New Jersey 08540

R. A. Smith
Westinghouse Astronuclear Laboratory
Pittsburgh, Pennsylvania

Introduction

The toroidal field coils of tokamak devices create a field within the torus whose strength varies inversely with distance from the machine center. This field, crossing the current in the TF coils, creates a magnetic pressure on the coil. The pressure produces a net inward centering force, countered by pressure on the wedge face, and a vertical separating force, causing tensile stress across the horizontal mid-plane. In the past these forces have been analyzed by superposition and beam theory.[1] Because of the size and complexity of the PLT machine it was decided to also initiate a finite element analysis of the coil. This paper describes both methods of analysis.

During a power test conducted in late 1974 and early 1975,[2] the toroidal fields were powered to 35 kilogauss, or 50% of full force. The deflections measured were much larger than predicted by either analysis. This was due in part to incomplete contact along the wedge faces, which introduced a non-linearity at low forces. However, the slope of the deflection-force curve at larger forces was also higher than predicted by either analysis, by factors of up to 7 and prompted a re-examination of both models.

The superposition model was modified through the inclusion of shear and tension effects. Calculation of a proper shear modulus was complicated by the layering of copper and epoxy. When this value was appropriately determined, as described below, the deflection output approximated the experimental data.

The finite element method of analysis is described for the toroidal field load conditions on the unsupported PLT toroidal field coil with special emphasis being placed upon model boundary conditions and assumed model material property formulations. The analysis results are shown to be very sensitive to the amount of contact area at the wedging interfaces of the TF coils and the location of contact between coils at the wedge face. Similarly, the finite element analysis results are shown to be sensitive to the material property assumptions regarding the alternating windings of copper and epoxy which form the coil. With the assumption of material isotropy, the finite element deflection predictions are in very poor agreement with the experimentally determined values. When material property modeling approximations are made to characterize the anistropy of the coil, the predictions can be made to agree with experimentally measured deflections by adjusting the value of the shear modulus in the laminate weak direction.

Experimental Results

Marino has described the basic set-up and results of the TF power test. The horizontal and vertical bore deflections were used as the primary points of comparison between predicted and measured deflections. These deflections were non-linear with force in the range below 10% of full force, but nearly linear with force between 10% and 50% of full force, as is shown in Figure 1, a typical curve of deflection vs. force.

In developing the superposition theory model, coil 4 was selected as typical, because at 25% of full force its horizontal and vertical deflections were within 0.001 inch of the average deflections for all coils. The increase in deflections between 10% and 50% force was then multiplied by 2.5 to give extrapolated full force deflections of .235 inch vertically and 0.143 inch horizontally.

In developing the finite element method model a different extrapolation was made. Coils 8 and 18 were taken as representative. These coils have above average deflections, and their deflections were more fully monitored for that reason. The tangent to the curve at 50% force was taken, and this slope was assumed to represent coil behavior. This would put the 100% force deflections in the range of .240 to .250 vertically and .112 to .138 horizontally. At 50% force a strain of 12,000 psi was recorded at the central mid-plane.

Beam Method

The basic method was described in reference (1) and consisted of numerically integrating beam equations along the arc of the coil mid-radius. The cross-sectional properties (area, moment of inertia) were calculated at each of the twenty points used in the integrations. The wedge forces that restrain the coils inward motion were modeled by 20 springs attached to the arc. The magnetic pressure was modeled as 20 point forces.

The program was written in Fortran format, using integrating and matrix solution sub- routines from IBM's Scientific Sub-Routine Package. As set-up and run at Princeton, on an IBM 360/95 the execution time was 16 seconds.

The original model gave forces, moments and stresses. It was later modified to provide vertical and horizontal diameter deflections as a basis for comparison with experimental data.

The model was then modified to include deflections due to tension and shear. This brought the model into reasonable approximation with the experimental results.

Two difficulties arose in picking a single value of shear modulus to represent the coil cross-section of layered copper and fiber-glass epoxy. The first problem was determining the correct way to combine the moduli of fiber-glass epoxy and copper. The second problem was determining the correct modulus for the epoxy-fiberglass.

Compression tests at Princeton determined E for the fiberglass -epoxy to be 1.14×10^6 psi.[3] This gives a shear modulus of 4.4×10^5 psi, assuming Poisson's ratio of 0.3. However, shear tests on a laminate buildup similar to the PLT coil layup indicate a shear modulus of 11×10^3 psi.[4] This agrees with data reported by M. Huguet of 8 kG/mm^2 or 11.3×10^3 psi.[5]

To combine the shear modulii of copper a and epoxy we define the effective shear modulus as the average shear stress divided by the shear deformation. The shear stress is equal transversely and longitudinally. The deformation is the sum of longitudinal and transverse components.

1) $G_{eff} = \tau / \alpha$

2) $\alpha = \alpha_L + \alpha_T$

The transverse deformation is inversely proportional to the sum of the products of modulus (G_e, G_c) and percentage of cross-sectional area, (Pe, Pc).

3) $\alpha_T = \dfrac{\tau}{2\,(Pe\ Ge + Pc\ Gc)}$

The longitudinal deformation is proportional to the sum of percentage areas divided by modulus.

4) $\alpha_L = \dfrac{\tau}{2} \left(\dfrac{Pe}{Ge} + \dfrac{Pc}{Gc} \right)$

With a little arithmetic we obtain:

5) $G_{eff} = 2 \left(\dfrac{Pe\ \ Ge + \ Pc\ Gc}{1 + Pe^2 + Pc^2 + Pe\ Pc \left(\dfrac{Gc}{Ge} + \dfrac{Ge}{Gc} \right)} \right)$

Taking for the TF coil Pe = .116, Pc = .884, and $G_c = 6.4 \times 10^6$ we get table (1)

Table 1

EFFECTIVE SHEAR MODULUS
VS
EPOXY SHEAR MODULUS (PSI)

G_{epoxy}	1.1×10^4	7.7×10^4	4.4×10^5	6.4×10^6
$G_{eff.}$	1.84×10^5	1.1×10^6	3.5×10^6	6.4×10^6

With other factors held constant the deflections predicted increase with decreasing shear modulus, with the ratio of vertical to horizontal deflection remaining constant. This is shown in Figure 2.

The ratio of vertical to horizontal diametral deflections decreases as the wedge "spring" stiffness is descreased. This is shown in table 2.

Decreasing the top height of the vertical wedge supports increases deflection. The ratio $R = \Delta D_y / \Delta D_x$ decreases at first but the full trend is unclear and was not fully explored. See Table 3.

The best fit to the experimental data extrapolated from coil 4 uses the full wedge face contact area, an effective shear modulus of 1.1×10^6 psi and the wedge stiffness calculated by including the effects of fiberglass laminations, insulation and cooling tubes. This predicts a full force vertical diameter deflection of .233 and horizontal diameter deflection of .143. The maximum stress predicted is 32 Ksi, without the center column. The maximum stress is at the midplane of the inner leg, and is caused by tension and bending.

Table 2

EFFECT OF WEDGE STIFFNESS
($G = 5.4 \times 10^5$ psi)

Run		Wedge Stiffness	$\Delta D_y / \Delta D_x$
6/03/75	III	1.00	1.72
6/10/75	II	.75	1.65
6/09/75	I	.50	1.56

Table 3

EFFECT OF WEDGE HEIGHT
($G = 4.0 \times 10^5$ psi)

Run		Wedge Height (in)	$\Delta D_y/\Delta D_x$
6/02/75	I	30.2	1.69
6/03/75	I	20	1.12
6/02/75	II	10	1.36

Finite Element Analysis Method and Result Comparisons

The finite element method of analysis was employed with the ANSYS general purpose computer program.[6] The three-dimensional isoparametric element was used to define a one-fourth geometric symmetric model of the toroidal field coil shown on Figure 3. The dividing planes for symmetry are the horizontal and vertical midplanes of the TF coil. The model was constructed with 25 finite elements per every four degree layer and with 45 layers of elements to span the π radians of the half coil. Two separate computer programs were used, one for the node point mesh and finite element generation,[7] and one for the force and displacement boundary conditions at the model node points.[8] The displacement boundary conditions were zero deflection at the horizontal midplane (Z = 0) in the direction normal to that plane, zero deflection at the vertical midplane (X = 0) in the direction normal to that plane, and zero deflection at the wedge face plane (X' = 0) over the assumed contact area in the direction normal to that plane. The computer program described in reference 8 computes the toroidal field and makes the vector cross product of the TF coil current with the field to evaluate the three components of force at every node in the current carrying portion of the toroidal field coil finite element model. The model shown here was constructed to allow for comparisons to be made for: (a) the effect of a low modulus epoxy material being present at the wedge interfaces between coils and at the interface between the two pancakes that form the entire coil, (b) the effect of the variation or the uncertainty of the amount of the wedge face contact area between the coils, and (c) the effect of anisotropy from the alternate layers of copper and epoxy in the coil winding. These were selected as variables for the present analysis when it was determined that a very simplified finite element model did not agree with the PLT experimentally measured TF coil deflections. This initial finite element approximation referred to as Computation (8) in reference 9 assumed the coil to be a homogeneous, isotropic structure with ideal wedge face contact. Only the Young's modulus was modified to reflect the relative proportions of copper and epoxy. For similar loading conditions, the experimentally measured coil diameter changes were about seven times that predicted by Computation (8) on the horizontal diameter, and about two and one-half times that predicted by Computation (8) for the vertical diameter. The wedge face contact area between coils was varied because light was seen through portions of this region on the PLT machine, at low field and the distribution of wedge face force is considered to have a significant influence upon the resultant diametral distortions of the coil. Furthermore, the non-flat wedge face surface is the only explanation that can be provided for the non-linearity of the experimental load deflection curves. It is hypothesized that as the centering force on the coil increases, so does the effective wedge face contact area; and as the toroidal field loads increase further, those regions that first make contact in the wedge area are loaded proportionately higher than if the contact area had been perfectly flat at first.

The amount of contact area and the location of the wedge contact area was controlled in the model by the node point selection for the boundary condition of no displacement normal to the wedge face. The assumed variations of wedge face contact area as related to the ideal surface with 100% contact is shown for the different models 8J through 8S on Figure 3.

The model for Computation 8 did not incorporate the thin layers of epoxy at the coil vertical interface planes shown on Figure (3) for the 8J through 8S models. The assumed Young's modulus for the epoxy was (1×10^6psi) 6.89 GPa. The material property assumptions for comparing the homogeneous isotropic modeling with an anisotropic approximation was the following: the model for Computations 8,8J, 8K, and 8M assumed the winding to be a homogeneous isotropic structure with a Young's modulus of (13.6×10^6psi) 93.9 GPa.

For all of the materials, the Poisson ratio was set at a 0.30 value. The models for Computations 8N, 8O, 8P, 8Q, 8R, and 8S assumed the windings to have different values of Young's modulus in the coil local R, θ, and X coordinate directions. In the θ and X-directions the alternating layers of copper and epoxy are acting in parallel. In the coil R direction, the material layering acts in series. Based upon the proportionate thicknesses of copper and epoxy the Young's modulus for the different directions were computed as:

6. E_R = 42. GPa (6.1×10^6 psi)

7. E_θ = 102. GPa (14.8×10^6 psi)

These properties were input to the finite element model in the global X, Y, Z coordinate system by defining 23 different materials for the finite element model as a function of the local coil angle, θ. Material number one occupied the regions defined by $0 \leq \theta \leq 4°$ and $176 \leq \theta \leq 180°$. Material number two occupied the regions defined by $4° \leq \theta \leq 8°$ and $172° \leq \theta \leq 176°$, and so on until material number twenty-three occupied the region defined by $88° \leq \theta \leq 92°$. The relationships used were:

8. $EX = EX$

9. $EY = ER + (E\theta - ER) \sin^2\theta$

10. $EZ = E\theta - (E\theta - ER) \sin^2\theta$

11. $GXY = \frac{EY}{2(1+\nu)}$; $GXZ = \frac{EZ}{2(1+\nu)}$

The value for the shear modulus, GYZ, was assumed to be the minimum value at all θ where it was further assumed that GYZ = GZY. Based upon the above modeling assumptions, the value for the shear modulus which was used in Computations 8N and 8P was:

12. $GYZ = 16.1$ GPa $(2.34 \times 10^6$ psi)

For the other computational models 8O, 8Q, 8R, and 8S, the value of GYZ was forced to take on different input values as a mechanism to make the predictions agree with the experimental measurements.

Table 4 provides the comparison between prediction models and the experimental measurements for a TF coil current of 31 kA which corresponds to 70% of rated current. The comparison between the finite element model predictions and the experimental measurements is actually a match of rate-of-change of deflection with respect to power at 50% full force (31 kA). This type of comparison is made because the model predictions are linear. The experimental deflection measurements on the PLT toroidal field coils were very non-linear with respect to load over the first 15 kA of power which corresponds to about 11% of full force, and this non-linearity appears to be non-existent at the higher power levels after the wedge face contact area becomes constant (by hypothesis). Further comparisons provided by Figures 4, 5, and 6 show the TF coil diametral deflections to be very sensitive to both the percent contact area at the wedge face and the assumed shear modulus, GYZ. The Computation 8S with 50% wedge face contact area, and with a shear modulus of GYZ = 10.3 GPa $(1.5 \times 10^6$ psi) gave the best experimental comparison. The slopes for some of the curves shown on Figures 4 and 5 where there is only a single data point were defined by recognizing that for a zero wedge face contact area the vertical diameter change of the coil should be approximately equal to the horizontal diameter change. This is reflected on Figure 6 by the trend that the ratio of the diameter changes is approximately 1.0 for no contact area on the wedge face. No contact area here means the coil is not wedging, but it is centering against a support column.

Figure 7 is a plot of an observed trend of predicted maximum stress versus the coil horizontal diameter change. Compared to the absolute value of experimental deflection at 31 kA the predicted stress is about 206 MPa (30,000 psi). A strain gage at that location during PLT power testing measured strains that would correspond to a stress of about 83 MPa (12,000 psi). Consequently there is wide disagreement between the finite element stress prediction and the reported strain gage measurement on PLT.

Conclusions

Both methods of analysis eventually produced close approximations to the experimental data. In both cases reduction of shear modulus was the key to proper modeling.

Other trends observed were:

1) an increase in deflection and decreased ratio of vertical to horizontal deflection, with wedge surface contact,

2) a decreasing ratio of vertical to horizontal deflection with decreasing wedge stiffness.

Acknowledgement

This work was supported by United States Energy Research and Development Administration Contract E(11-1)-3073.

References

1. J. Frankenberg, J. Citrolo, P. Bonanos, PLT Confining Field Coil Loading and Stresses, Fifth Symposium on Engineering Problems of Fusion Research, Princeton, New Jersey, November 1973 (IEEE N.Y. PP 332-334.

2. R. Marino, J. Citrolo, J. Frankenberg, PLT Toroidal Field Coil Power Test, Proceedings of Sixth Symposium on Engineering Problems of Fusion Research San Diego, California, November, 1975, to be published.

3. C. Bushnell, Compression Tests of PLT Insulation System, private communication, Plasma Physics Laboratory, Princeton, New Jersey, 08540 5 March 1973.

4. R. Marino, Shear Properties of a PLT TF Coil Epoxy Laminate, private communication, Plasma Physics Laboratory, Princeton, New Jersey, December 1973.

5. M. Huguet, private communication to J. Citrolo, April 1975.

6. J.A. Swanson, G.J. DeSalve, ANSYS Engineering Analysis Systems User's Manual October 1, 1972, Elizabeth, Pennsylvania 15037.

7. R.A. Smith, Finite Element and Node Point Generation Computer Programs Used for the Design of Toroidal Field Coils in Tokamak Fusion Devices, WFPS-TME-001, June 30, 1975, Westinghouse Electric Corporation.

8. R.A. Smith, Field Load and Displacement Boundary Condition Computer Program Used for the Finite Element Analysis and Design of Toroidal Field Coils in a Tokamak, WFPS-TME-002, June 30, 1975, Westinghouse Electric Corporation.

9. R.A. Smith, The Toroidal Field Coil Stress Analysis Method and Results for the Princeton PDX and PLT Controlled Fusion Experiment., WANL-TME-2860, June 30, 1974, Westinghouse Astronuclear Laboratory.

Table 4

FINITE ELEMENT MODEL RESULT COMPARISONS WITH EXPERIMENTAL MEASUREMENTS

Model Number	Wedge Area (in.)	Predictions				
		GYZ x 10^6 (psi)	ΔD_H (in.)	ΔD_V (in.)	$\frac{\Delta D_V}{\Delta D_H}$	SZ (psi)
8	92%	5.23	0.009	0.052	5.44	12,200
8J	86%	5.23	0.012	0.054	4.30	13,000
8K	34%	5.23	0.074	0.094	1.27	26,000
8L	34%	5.23	-0.019	0.034	-1.76	7,000
8M	34%	5.23	0.035	0.069	1.97	17,800
8N	86%	2.34	0.011	0.074	6.57	15,000
8O	86%	0.106	-0.053	0.578	-10.7	28,000
8P	34%	2.34	0.085	0.115	1.35	28,800
8Q	50%	1.00	0.063	0.148	2.35	24,500
8R	56%	1.40	0.050	0.121	2.41	21,700
8S	50%	1.50	0.059	0.122	2.06	23,045

ΔD_H = Contraction of the horizontal inside diameter
ΔD_V = Expansion of the vertical inside diameter
SZ = Axial stress at the location shown on Figure 7

	Experimental Measurements		
	ΔD_H (in.)	ΔD_V (in.)	$\frac{\Delta D_V}{\Delta D_H}$
Absolute, Coil 8	0.078	0.144	N/A
Slope, Coil 8	0.056	0.125	2.22
Absolute, Coil 18	0.098	0.136	N/A
Slope, Coil 18	0.069	0.120	1.75

Absolute = The total measured deflection
Slope = The change of deflection over the power range for the straight line tangent to the experimental load deflection curve at the point of maximum power

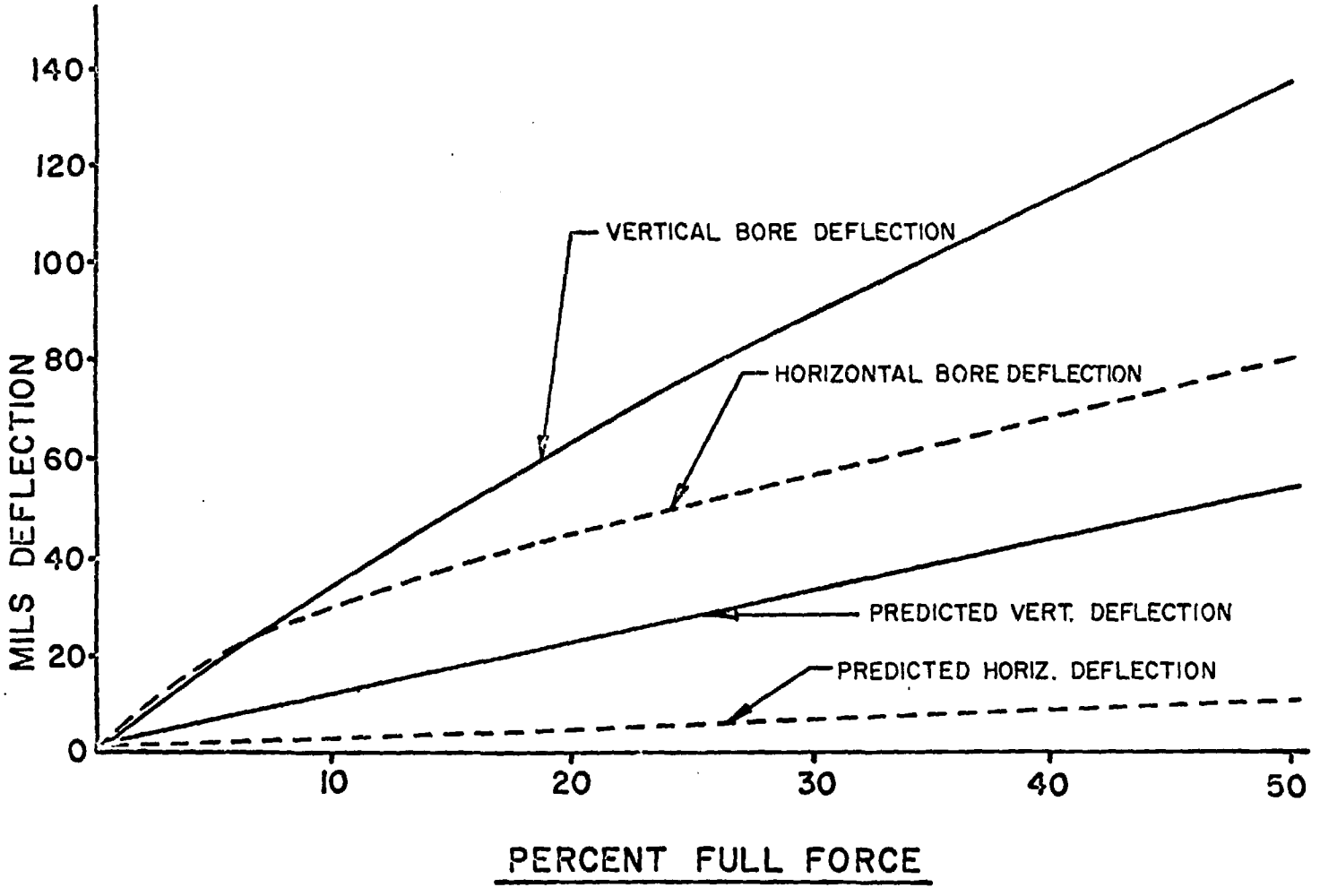
140
120
100
80
60
40
20
0
MILS DEFLECTION
VERTICAL BORE DEFLECTION
HORIZONTAL BORE DEFLECTION
PREDICTED VERT. DEFLECTION
PREDICTED HORIZ. DEFLECTION
10
20
30
40
50
PERCENT FULL FORCE

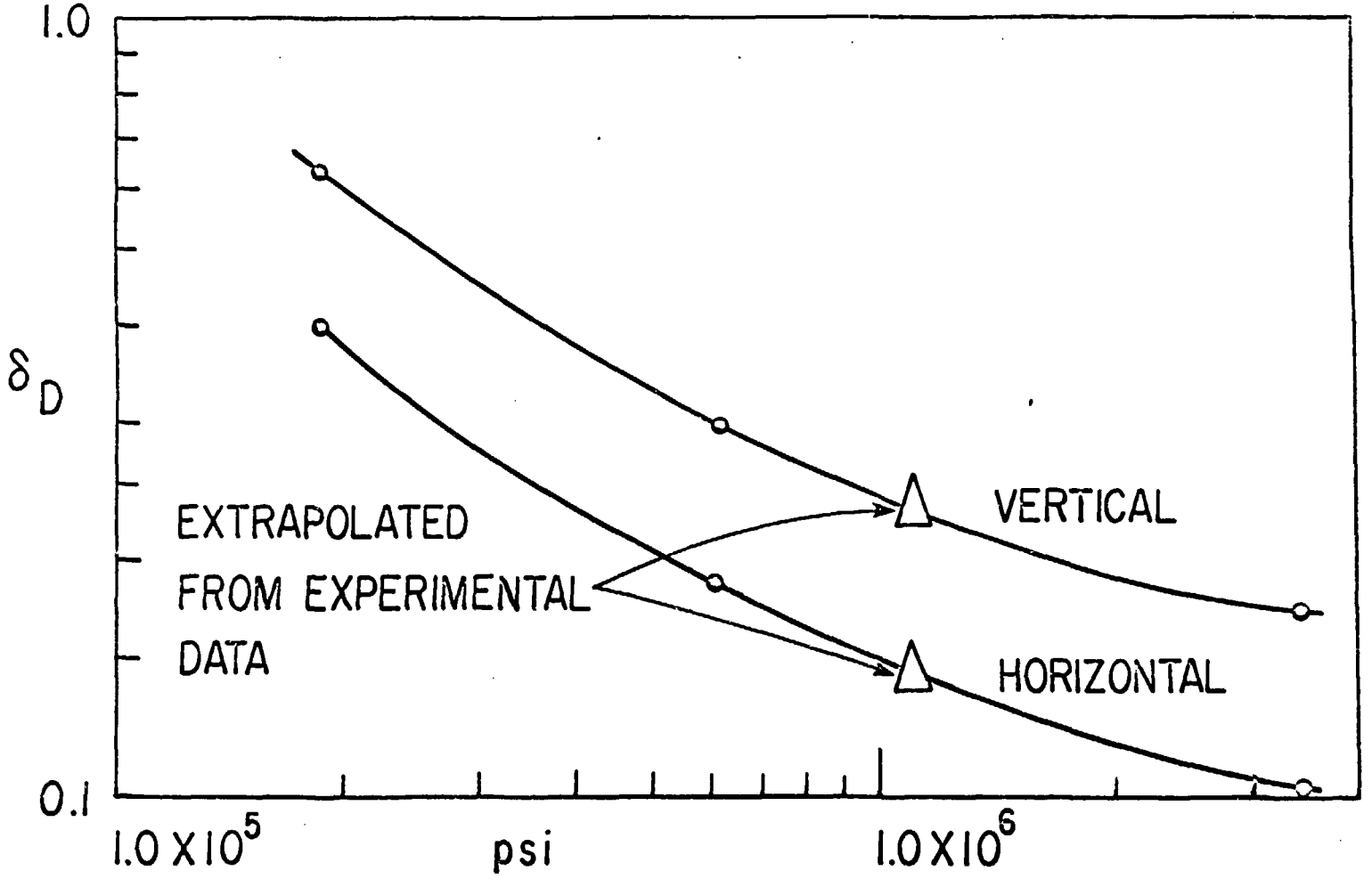
1.0
δ_D
0.1
EXTRAPOLATED
FROM EXPERIMENTAL
DATA
VERTICAL
HORIZONTAL
1.0×10^5
psi
1.0×10^6

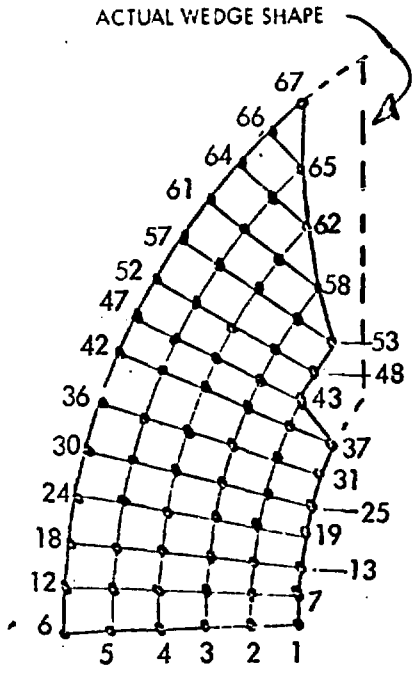

Model Number	% of Actual Wedge Areas	Nodes with UX' = 0
8J	86%	1 to 67
8K	34%	1 to 30
8L	34%	30, 35, 36, 40, 41, 42 44 to 47, 49 to 67
8M	34%	3 to 6, 9 to 12, 15 to 18, 22, 23, 24, 28, 29, 30, 34, 35, 36, 40, 41, 42, 46, 47, 51, 52, 57
8N	86%	1 to 67
8O	86%	1 to 67
8P	34%	1 to 30
8Q	50%	1 to 42
8R	56%	1 to 42, 44, 45, 46
8S	50%	1 to 42

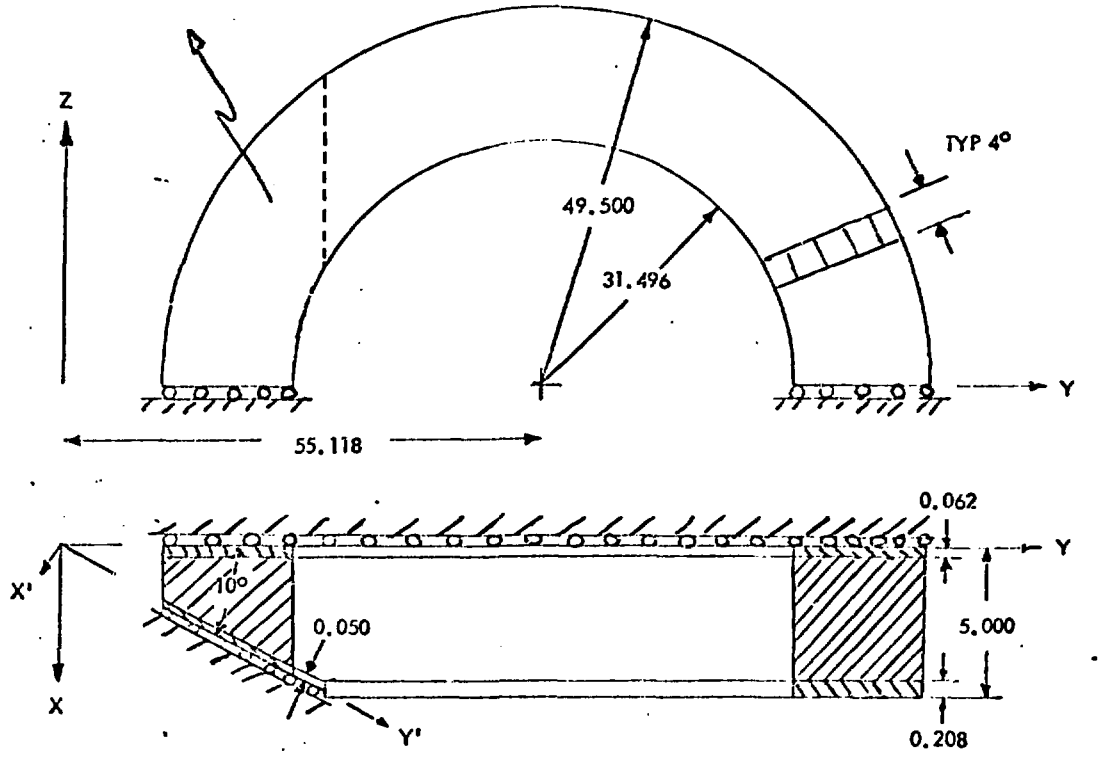

Fig. 3 The PLT Toroidal Field Coil One-Fourth Geometric Symmetric Finite Element Model with Indicated Boundary Conditions for Toroidal Field Load Stress Analysis

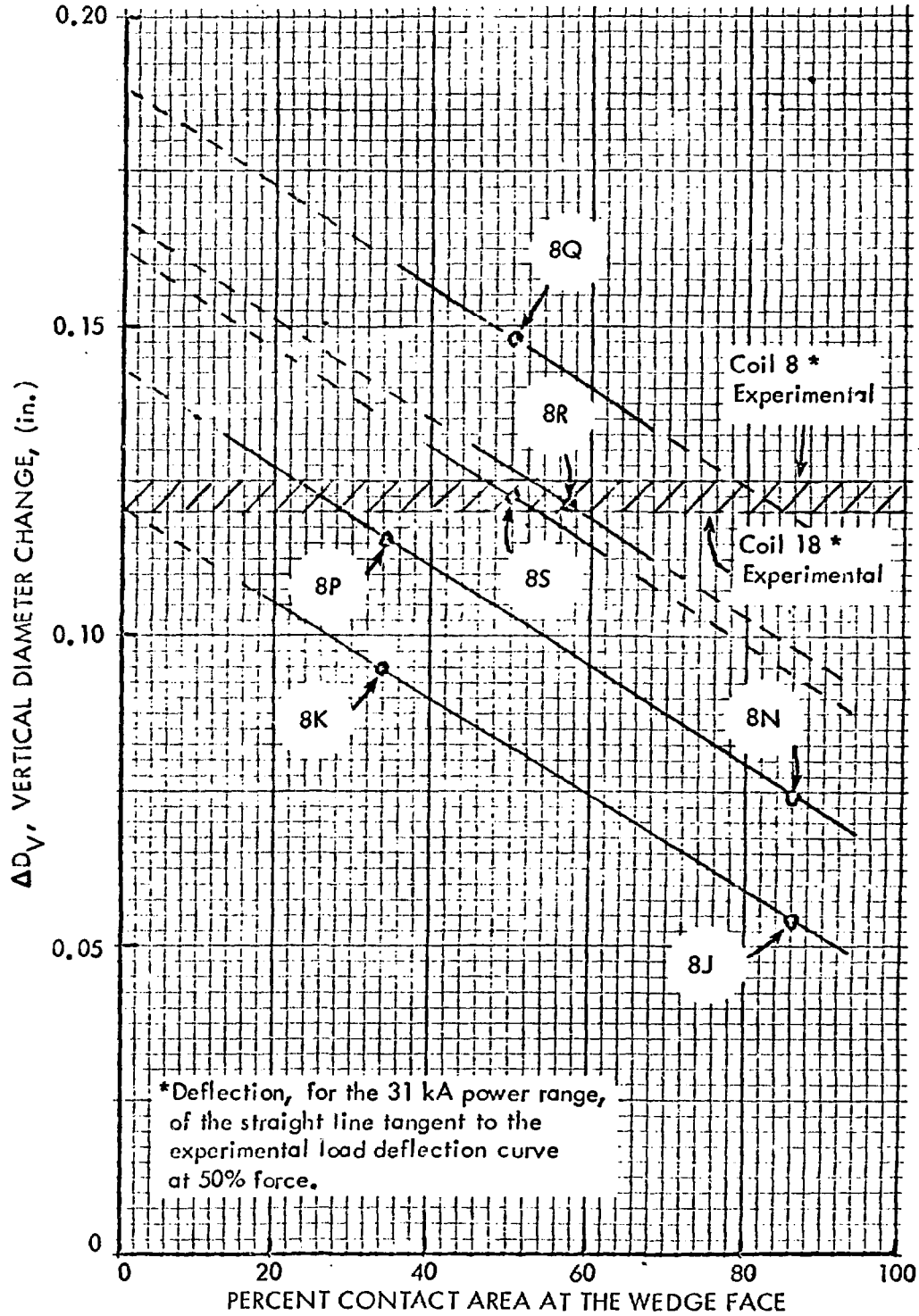

Fig. 4 Finite Element Model Predictions of TF Coil Vertical Diameter Deflections at 50% Toroidal Field Force

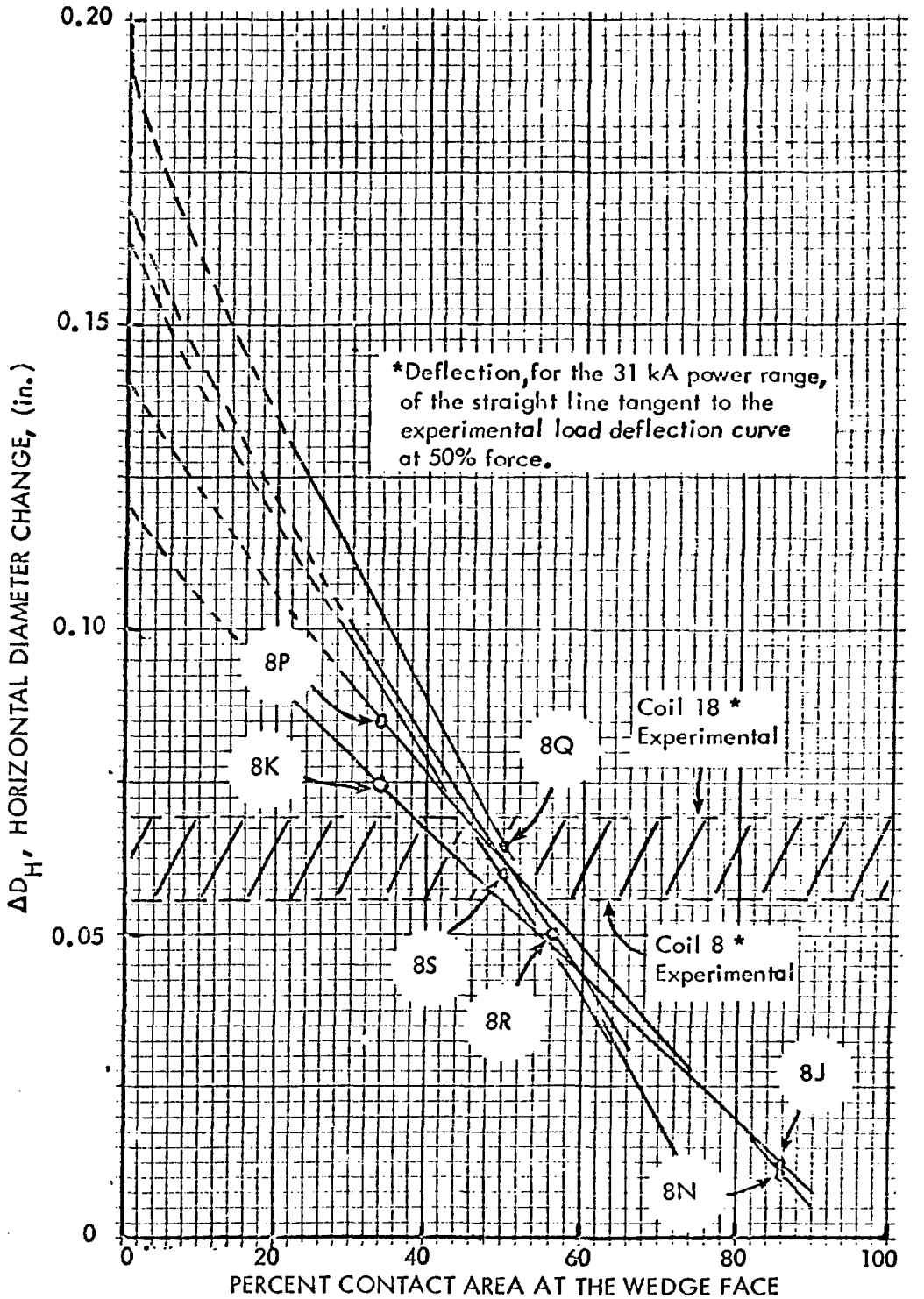

Fig. 5 Finite Element Model Predictions of TF Coil Horizontal Diameter Deflections at 50% Toroidal Field Force

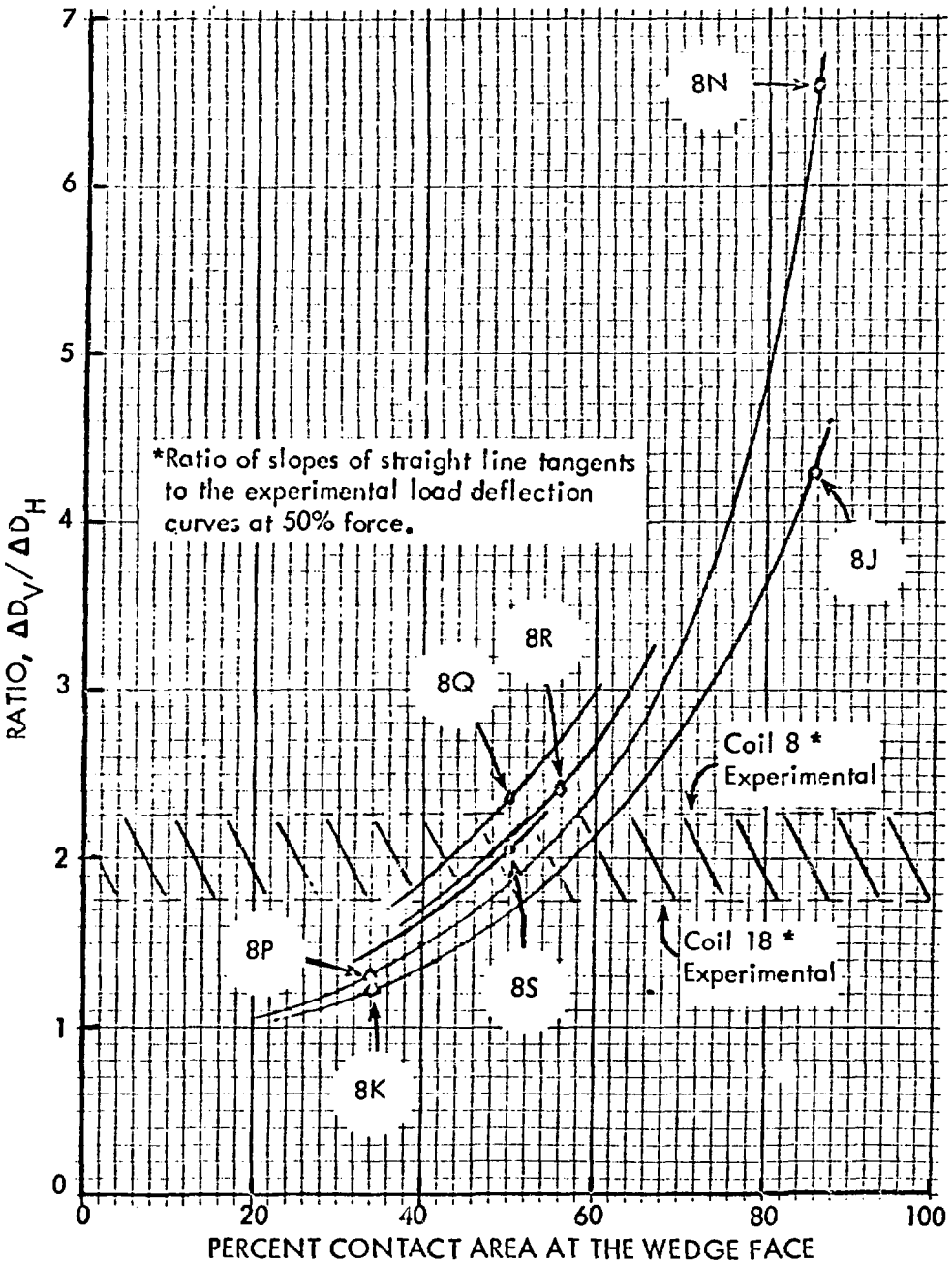

Fig. 6 Finite Element Model Predictions for the Ratio of TF Coil Vertical to Horizontal Deflections at 50% Toroidal Field Force

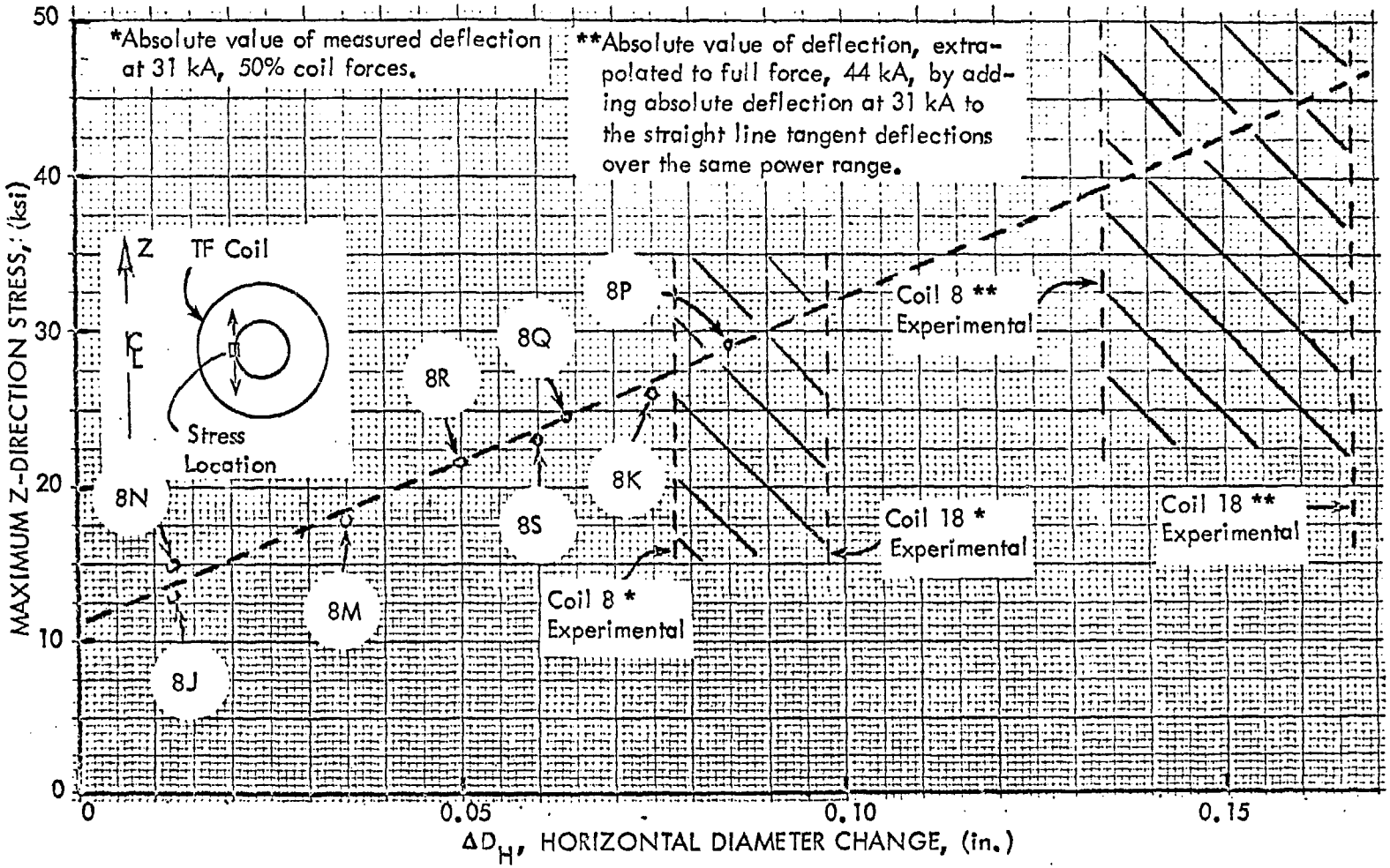

Fig. 7 Finite Element Model Maximum Stress Predictions for the PLT Toroidal Field Coil